DL/SCI/TM78E

technical memorandum Daresbury Laboratory

DL/SCI/TM78E

A TWIN FREQUENCY MODULATION TECHNIQUE FOR RETARDING FIELD ANALYSERS

by

P. BAILEY and R.A. HEARSEY, SERC Daresbury Laboratory

Lending Copy

June, 1991

Science and Engineering Research Council
DARESBURY LABORATORY
Daresbury, Warrington WA4 4AD

ISSN 0144-5677

A Twin Frequency Modulation Technique for Retarding Field Analysers

Paul Bailey and R. A. Hearsey
S.E.R.C. Daresbury Laboratory

Abstract

We present here a report on a novel modulation technique for use with retarding field analysers. The more common technique employs a system which uses a high-Q filter to discriminate between an unwanted frequency 'f' and a wanted frequency of 2f. For technical reasons it is desirable to lower the Q of this filter. The twin frequency technique can employ frequencies separated by several orders of magnitude thus reducing the required 'Q' of the filter. It also has the advantage that, to a first approximation, it should produce a twofold increase in signal level.

1. Introduction

Surface science experiments generally require that the surfaces to be investigated be; (i) clean and (ii) structurally well ordered. The low energy diffraction technique (LEED) is a convenient and popular technique for assessing surface structure. The cleanliness of a surface can readily be assessed by monitoring the levels of common contaminats such as carbon, oxygen and sulphur via Auger spectrometry. A modified LEED system may also be used for Auger analysis (ref. 1) in the form of a retarding field analyser (RFA), shown schematically in fig. 1. An RFA is expected to have an instrumental linewidth of about 0.5% in the case of a four grid system and around five times that for a three grid system (ref. 2). An Auger system based on LEED optics is therefore a particularly appropriate and useful tool for surface science experiments and the combination of the two techniques within the same physical housing is an efficient use of valuable space in an experimental vacuum chamber. This report describes a novel modulation technique for use with RFA systems. The reason for investigating a different RFA analysis technique is that the standard technique employs a system which uses a high-Q filter to discriminate between an unwanted frequency 'f' and a wanted frequency of 2f. However, due to this high 'Q' low frequency noise can cause the filter to ring at the detection frequency of 2f. Thus, random noise which would otherwise be rejected by the lock-in amplifer is converted by the high-Q filter into a synchronous signal and detected by the lock-in. In order to eliminate this effect the 'Q' of the filter needs to be reduced. The twin frequency technique can employ frequencies separated by several orders of magnitude thus reducing the required 'Q' of the filter. It also has the advantage that, to a first approximation, it should produce a twofold increase in signal level.

2. RFA energy analysers

An RFA energy selects by use of a biassed grid through which the electrons to be analysed must pass. Electrons with energy greater than the bias are transmitted, those with less are reflected. The transmitted intensity of electrons is thus composed of <u>all</u> electrons with energy greater than the bias and an RFA energy spectrum produced by scanning the bias is an integral energy distribution. Deconvolution of this integral function by differentiation is a necessary feature of the analysis and is usually carried out electronically. However it has been shown that spectrum detectability can be greatly enhanced by differentiating the signal a second time (ref. 3)., again this can be effected electronically.

3. Electronic Differentiation

Electronic differentiation operates by mixing a small a.c. signal of frequency 'F' with the bias voltage applied to the grid. This a.c. signal modulates the transmitted beam. At any bias voltage (B) the transmitted electron intensity is modulated by the a.c. signal (VsinF) which sweeps the bias over the full peak to peak voltage of the a.c. modulation. The transmitted signal is thus composed of the integral energy distributions' value at a bias voltage B, $(I\{E\}_B)$, and a component affected by the modulation. The measured signal S is thus given by;

$$S = f(I\{E + V\sin F\}_B)$$

The Taylor expansion of f(a+x) is;

$$f(a+x) = f(a) + f^{i}(a)x + f^{ii}(a)x^2/2 + f^{iii}(a)x^3/3! + f^{iv}(a)x^4/4! \text{ etc.} \quad .....1$$

In our case the first derivative term is $I^{i}\{E\}_B V\sin F$.
Thus the component of the transmitted signal which has a frequency F is proportional to the first derivative of the integral energy spectrum, i.e. proportional to the initial energy spectrum. In practice, therefore, selecting this frequency component produces a signal proportional to the initial electron energy distribution at that bias voltage. However, when looking at small peaks superimposed on a slowly varying background their presence can be made clearer by differentiating the signal. In our case this would be a second differentiation. To see how this may be achieved we look back to the second derivative term in eqn. 1. This term has an x^2 (i.e. $\sin^2$) component and using the identity;

$$\sin^2\theta = 1/2(1 - \cos 2\theta)$$

the term becomes;

$$f^{ii}(a)x^2/2 = I^{ii}\{E\}_B V^2/4(1 - \cos 2F) \quad .....2$$

Therefore selecting a component of frequency 2F produces a signal which is proportional to the second derivative of the integral energy spectrum, or the first derivative of the initial energy spectrum. Selecting a frequency of 2F thus performs two stages of differentiation, the first removes the integrating effect of the RFA technique, the second enhances the peak to background level. This f, 2f technique we shall call the standard RFA technique.

The alternative method of producing a second derivative is to employ twin modulation frequencies (F_1, F_2) which have a small frequency difference. The parameter 'x' in eqn. 1 now becomes

$x = V(\sin F_1 + \sin F_2)$ and the second derivative term becomes;

$$f^{ii}(a)x^2/2 = I^{ii}\{E\}_B V^2/2(\sin F_1 + \sin F_2)^2 \quad .....3$$

Looking only at the sine terms and expanding;

$$(\sin F_1 + \sin F_2)^2 = \sin^2 F_1 + \sin^2 F_2 + 2\sin F_1 \sin F_2 \quad .....4$$

Using the identity;

$$2\sin A\cos B = \cos(A+B) - \cos(A-B) \quad .....5$$

and substituting eqn. 5 into eqn. 4;

$$(\sin F_1 + \sin F_2)^2 = \sin^2 F_1 + \sin^2 F_2 + \sin(F_1 + F_2) + \sin(F_1 - F_2)$$

substituting this into eqn. 3;

$$f^{ii}(a)x^2/2 = I^{ii}\{E\}_B V^2/2\{\sin^2 F_1 + \sin^2 F_2 + \sin(F_1 + F_2) + \sin(F_1 - F_2)\} \quad .....6$$

Therefore selecting a frequency of $(F_1 - F_2)$ produces a signal proportional to the second derivative as before. This technique using two similar modulation frequencies we shall call the twin frequency technique. Interestingly eqn. 6 predicts a signal level twice as large as that predicted by the single frequency (standard) technique in eqn. 2. Assuming that noise is external this means that the twin frequency technique could have a x2 improvement in signal to noise ratio and hence a x2 improvement in scan speeds.

However, in both cases there are higher order terms in eqn. 1 which contribute to the frequency of interest. A more accurate analysis requires that these contributions be evaluated and in order to do this we shall assume that the initial energy distribution (i.e. the first derivative of I{E})is composed of a peak of Gaussian shape.

(i) Standard RFA

The amplitude of the 2F component using the first six terms calculated from eqn. 1 is;

$$A_2 = I^{ii}\{E\}_B V^2/2!\,(4/8) + I^{iv}\{E\}_B V^4/4!\,(8/16) + I^{vi}\{E\}_B V^6/6!\,(15/32) + I^{viii}\{E\}_B V^8/8!\,(28/64) + I^{x}\{E\}_B V^{10}/10!\,(53/128) + I^{xii}\{E\}_B V^{12}/12!(93/256)$$

The general form is;

$$A_2 = \sum [\, I^{n}\{E\}_B k_n V^n/n! \,] \quad .....7$$

where n is even and k_n is given by;

n =	2	4	6	8	10	12
k_n =	4/8	8/16	15/32	28/64	53/128	93/256

The effect of the derivative $(I^n\{E\}_B)$ can be found by successive differentiation of the Gaussian function which is;

$G(x) = \exp-(1/2\{x/\sigma\}^2)$ (N.B. $G(x) = I'\{E\}_B$)

We cannot use the value of the differential at x=0 as this is always zero for the order of the differentials in eqn. 7. We shall therefore evaluate the differential at another arbitrary but convenient point, x=σ. A general expression for the value of the n^{th} differential is;

$G^n = x^{(n-1)}/\sigma^{2(n-1)}\, G_n \exp-(1/2\{x/\sigma\}^2)$

and at x=σ is:

$$G^n = \{1/\sigma\}^{(n-1)}\, G_n \exp\ (-0.5) \qquad .....8$$

where G_n is a constant given by;

n =	2	4	6	8	10	12
G_n =	1	-2	6	-20	28	-936

Combining eqns. 7 and 8 gives;

$$A_2 = \sum [\ \{V/\sigma\}^{(n-1)}\ V\ G_n k_n/n!\ \exp\ (-0.5)\ ] \qquad .....9$$

where n is even.

(ii) Twin frequency RFA

In a similar manner expressions for the first six terms describing the difference frequency can be calculated.

$$A_{diff} = \sum [\ \{V/\sigma\}^{(n-1)}\ V\ G_n k_n/n!\ \exp\ (-0.5)\ ] \qquad ...10$$

where n is even, G_n is given above and k_n is given by;

n =	2	4	6	8	10	12
k_n =	1	2	9/4	5/2	175/64	198/65

It is evident that eqns. 9,10 are identical and simply have different values of the constant K_n. Figure 2 compares the sensitivity of the two techniques, i.e. eqns. 9 and 10, to a first approximation and also including the six terms given above.

(iii) The effect of peak broadening

Eqns. 9 and 10 above predict the amplitude as a function both of the modulation voltage and the initial peak width (σ). However, for modulation voltages greater than the initial peak width the apparent peak width is broadened by the effect of the modulation. A model which quantifies the peak broadening due to modulation is developed in appendix B. The main result of this model is that the observed peak width approximately increases in proportion to the modulation voltage;

$$\sigma = (\ \Delta E^2 + k_2^2 V_p^2)^{0.5} \qquad ...11$$

where ΔE is the initial peak width, k_2 is a constant and V_p is the modulation peak voltage.

Substituting eqn. 11 in eqn. 9 gives an expression for the peak amplitude as a function of modulation only;

$$A_2 = \sum [\ I_o\{V/(\ \Delta E^2 + k_2^2 V_p^2)^{0.5}\}^{(n-1)}\ V\ G_n k_n/n!\ \exp\ (-0.5)\ ] \quad ...12$$

We can see the effect this has by considering large modulation values where $V_p >> \Delta E$;

$$A_2 = \sum [\ I_o\{1/k_2\}^{(n-1)}\ V\ G_n k_n/n!\ \exp\ (-0.5)\ ] \qquad ...13$$

This expression shows that peak amplitude increases linearly with modulation voltage (V) for values of V>>ΔE. This applies equally to the twin frequency case.

4. Comparison of Standard and Twin Frequency RFA

In this comparison we have used the two RFA techniques to energy analyse the so-called primary peak in the electron energy spectrum. This peak is produced when primary electrons bombarding the target are elastically backscattered from electrons in the target. fig. 3 shows the primary peak obtained using the standard RFA technique including, for reference, the first differential signal, i.e. the initial energy spectrum. The primary peak was chosen in preference to Auger peaks for two reasons, (i) the signal levels from the primary peak are greater than from Auger peaks which allows a greater range of modulation levels to be used and (ii) this peak is less sensitive to surface contamination than the Auger peaks and so provides a more stable basis for the comparison.

The experimental set-up for this comparison was as follows. The LEED optics was a Vacuum Generators 4 grid forward view LEED with a 326 control unit. The trap current was set to 200 μA which resulted in around 2μA current on an unsuppressed copper target. The geometry was normal incidence, primary energy was 1 keV, the screen bias voltage was +300 V, and the lock-in amplifier was a Brookdeal type 9503. The vacuum system was ion pumped and the experiments were carried out at a pressure of 10^{-8} mbar. The sample was high purity polycrystalline copper cleaned by ion bombardment and annealled. The standard RFA employed 2.375 kHz modulation and 4.75 kHz detection frequencies, whilst the twin frequency RFA employed 68.27/65.54 kHz modulation and 2.73 kHz detection frequencies.

A comparison of the two techniques was carried out by recording the primary peak as a function of modulation level. As the modulation is increased two things occur (i) the signal level of the peak increases and (ii) the energy width of the peak increases. fig. 4 shows peak width as a function of modulation voltage and fig. 5 shows peak height versus modulation. The quoted levels refer to the current monitored at the screen, i.e. at the input of the pre-amplifier (input impedance 1 kohm). The two main features of these two figures are (i) fig. 4 shows that the same modulation level does not cause the same amount of peak broadening and (ii) the twin frequency technique produces a larger signal (as predicted by eqns. 2, and 6). An explanation of the criteria used to measure the peak width and height is given in appendix A.

5. Discussion

Referring to fig. 4; for both techniques the same amount of modulation should produce the same amount of peak broadening, however it does not appear to although it is possible that our calibration of the two waveforms is incorrect. If we compare an ideal twin frequency waveform generated numerically (fig. 6) with an actual waveform measured at the output of our twin frequency generator (fig. 7), we can see that there is some difference in the sharpness, or height, of the wave envelope, possibly due to non-linearities in the power amplifier which can clearly be seen at the highest modulation settings. The standard technique by contrast uses a pure sine wave modulation which is more easily characterised. We shall therefore re-calibrate our twin frequency modulation values to cause the points in fig. 4 to lie on one line. This is shown in figure 8 where the twin frequency modulation values have been reduced by a factor (0.86) chosen to match the points over the middle of the modulation range.

Eqn. B.3 in Appendix B predicts the variation in peak width (σ) as a function of modulation;

$$\sigma = (\Delta E^2 + k_2^2 V^2)^{0.5} \quad \ldots 14$$

where V is the peak modulation voltage and k_2 is expected to be

unity.

The 'y' intercept in fig. 4 suggests that the instrumental linewidth (ΔE) is about 1.8 eV. At an analyser energy of 1kV a 1.8V error corresponds to an instrumental resolution of 0.18% which is agrees with the manufacturers' specification. The prediction shown in fig. 8 is a plot of eqn. 11 with ΔE=1.8 eV but with k_2 = 0.71. This value for k_2 is thus significantly different from the value of 1.0 predicted by the model in appendix B. The physical implication is that the applied modulation, V, has an effective value of only 0.71xV and this appears valid for both the systems.

Eqn. 13 describes the variation in peak intensity as a function of modulation (V). Fig. 9 is fig. 5 redrawn for the re-calibrated modulation values and shows the relative peak intensities as a function of modulation. The prediction shown in fig. 9 is eqn. 13 with the following values;

ΔE=1.8 eV and k_2 = 0.71. The y-axis has been matched to the twin frequency data points.

The agreement seen in fig. 9 is fair in both cases below 2V modulation. Above 2V modulation the twin frequency agrees well but the standard is progressively lower than the prediction. The magnitude of the theoretical slope at these higher modulation values is determined by two main effects ; (i) the shape of the original peak whose higher order differentials determine the G_n constants in eqns. 9,10 and (ii) the relationship between the peak width and the applied modulation i.e. the value of the constant k_2. The good fit seen in fig. 8 indicates that the relationship between the width and the modulation is well behaved over this region and so (ii) is unlikely to be producing the behaviour seen in fig. 9. Effects due to peak shape are a more likely candidate since the primary peak has a number of features which merge at the higher modulation levels. Despite the quantitative differences in fig. 9 the general trend of the experimental and theoretical curves is very similar and the overall agreement is fair. Interestingly there is an almost constant factor of two increase in peak amplitude between the twin frequency and the standard data over the whole modulation range.

Although the twin frequency system gives a twofold increase in signal, the parameter which determines a techniques' usefulness is signal to noise ratio (S/N ratio). Whilst quantitative measurement of noise is difficult the noise at the output of both systems is of a similar level. This noise has a characteristic 1/f frequency spectrum and is largely independent of the main experimental parameters, i.e. modulation and primary current. This suggests that the origin of the noise is external to the electron signal, i.e.

electronic noise due to the pre-amplifier or lock-in amplifier. Hence it appears that the S/N ratio for the twin frequency technique is a factor of two better than the standard technique. An important difference exists between the two techniques at the detection stage. In the case of the standard technique the wanted signal is higher in frequency than the unwanted (modulation) signal by an even factor (two). This means that the modulation signal will be averaged to zero by the lock-in amplifier provided a suitably long time constant is selected. However, in the TF case the wanted signal is of lower frequency than the unwanted signal and so will be detected by the lock-in amplifier and cannot be removed by smoothing at this stage. This means that some degree of filtering is still necessary before the lock-in. But the comparatively large frequency difference in the TF case means that the effect of smoothing before the lock-in is to attenuate the unwanted signal by the ratio of the frequency difference.

6. Conclusions

(i) an RFA electronic differentiation system based on twin modulation frequencies has been operated successfully.

(ii) both techniques exhibit a unit increase in peak width per 0.71 volt of peak modulation. This is in contrast to a prediction of a unit increase per unit of peak modulation. This may be an indication of reduced modulation field in the grid region due to field penetration of the grids. A similar investigation carried out on a three grid LEED system may illuminate this matter.

(iii) the signal amplitude from the twin frequency system is a factor of two greater than for the standard single frequency system for the same level of modulation and hence the same amount of peak broadening. Whilst this is not in quantitative agreement with the prediction the general shapes of the experimental and theoretical curves are a good match.

(iv) the practical gain from (iii) above depends upon the relative amounts of noise in each case, i.e. the signal to noise ratio for each technique. This is virtually impossible to measure accurately. Our estimates are that the twin frequency signal to noise ratio is a factor of two greater than that of the standard system. Following from (iii) above, this implies that the noise levels are similar for the two techniques.

(iv) investigations into possible sources of noise suggest that whilst some noise can be traced to the pre-amplifier the majority of noise is produced by the lock-in amplifier.

7. Recommendations

(i) investigations into the lock-in amplifier noise indicate a

typical 1/f noise spectrum. However, the electronics unit which generates the twin frequencies was designed to have a difference frequency almost half the operating frequency of the standard system. Thus, in view of a 1/f noise spectrum, a direct comparison of the noise of the two systems is difficult. However, significantly increasing the difference frequency should move the operating point along the noise spectrum and reduce the noise level.

(ii) the twin frequencies used were around 68 kHz with a difference of around 2.7 kHz, i.e. separated in frequency by a factor of 25. In order to prevent the high frequencies saturating the lock-in amplifier, a high-Q filter with a performance comparable to that used in the standard system was still required. Increasing these frequencies to the highest practicable limit would lessen the need for a high-Q filter. However this action is to some extent incompatible with (i) above and so an arrangement similar to the standard RFA may be required in which a small amount of the modulation is phase shifted by 180° and added to the detector input.

(iii) in view of point 6(iv) above it should be useful to construct a lock-in amplifier whose design would be tailored to an RFA Auger system. This would result in a lock-in amplifier with the minimum of features, i.e. filters, options etc., and hence a minimum amount of electronic noise.

8. Acknowledgements

The authors are grateful to D. S-L. Law and D. Teehan for useful discussions.

9. References

1. L.B.Leder and J.A.Simpson, Rev. Sci. Instrum. 29, 571 (1958)
2. N.J.Taylor, Rev. Sci. Instrum. 40, 792 (1969)
3. L.A.Harris, J. Appl. Phys. 39, 1419 (1968)

10. Figure captions

1. A schematic of a 'standard' RFA Auger system.
2. A comparison of the sensitivity of standard and twin frequency RFA Auger.
3. An illustration of electronic differentiation used in RFA Auger.
4. The energy width of a 1kV elastic peak as a function of modulation level.
5. The amplitude of a 1kV elastic peak as a function of modulation level.
6. An ideal twin frequency modulating waveform.
7. An actual twin frequency modulating waveform.
8. Fig. 4 with the twin frequency modulation reduced by 0.86.

9. Fig. 5 with the twin frequency modulation reduced by 0.86
10. An illustration of peak width measurement.
11. The effect of modulation on the transmission of monoenergetic electrons in an RFA.
12. The transmission function of an RFA with modulation.
13. The calculated RFA output for an initial Gaussian energy distribution with and without modulation.
14. The calculated peak broadening due RFA modulation.

Appendix A

Measurement of peak parameters

Accurate measurement of the height and width of the type of peak shown in figure 3 requires that measurements be made only from well defined points on the peak. Fig. 10 illustrates both the height and width measurement. It is evident that the datum points of both the zero crossing point and the turnover point are well defined and the peak height is simply measured from the zero line to the peak. The peak width is measured from the minimum of the derivative curve to the crossover point. The sigma illustrated in fig. 10 is thus a half-width measurement and for a Gaussian peak is equal to the standard deviation.

Appendix B

Peak width as a function of modulation level

Applying modulation to the retarding grid simply scans the analysing voltage over a small range. If we consider a delta function signal of energy 'E_d' in the range covered by the modulation, as shown in fig. 11 Then the signal is retarded whenever the modulation is greater than E_d and is transmitted for the time when the modulation level is less than E_d. The ratio of these two times gives the extent to which the delta function is attenuated by the modulation, i.e. for an E_d equal to the mean modulation level the signal is transmitted for 50% of the time. An expression may be deduced from fig. 11 for the transmission of any particular E_d ;

$$T = 0.5 + \sin^{-1}(E/V_p)/180 \qquad ..B.1$$

where E = the difference between E_d and the modulation mean
V_p = the modulation peak voltage,
and T = unity for $E > +V_p$
$T = 0$ for $E < -V_p$.

We can apply this principle to an RFA spectrum by considering the transmission of the delta function as the analyser energy is swept through the range covered by the modulation. Fig. 12 shows the transmitted signal with and without modulation and it is apparent that the energy spread caused by the modulation is approximately equal to the peak voltage. Whilst fig. 12 shows the simple case of a single energy delta function an extended energy distribution may be constructed from a number of delta functions of differing energies. The transmitted energy distribution is then the sum of all the components, each of which has an energy distribution of the type shown in figure 12. In order to examine the effect the modulation has on an energy distribution the result can be differentiated twice to obtain the type of peak which may be observed experimentally and the result can be seen in fig. 13 for an initial Gaussian distrbution of σ=1 V and modulation of 1V peak. A number of such cases have been considered and fig. 14 shows the increase in peak width of a Gaussian energy distribution (σ=1) as a function of peak modulation voltage. The theoretical width shown in fig. 14 has been calculated from the following equation on the assumption that the initial sigma and the modulation broadening add in quadrature i.e.;

$$\sigma_{eff} = (\sigma^2 + k_2^2 V_p^2)^{0.5}$$

where $\sigma = 1$

Thus in a practical situation we expect that the observed peak width will increase in proportion to the modulation voltage but also note that there may be a measurable contribution (ΔE) from the initial energy spread of the primary electron beam or due to the instrumental resolution i.e.;

$$\sigma = (\Delta E^2 + k_2^2 V_p^2)^{0.5} \qquad ..B.3$$

where V_p is the peak modulation voltage and k_2 is unity

Figure 1

Schematic of standard Auger system

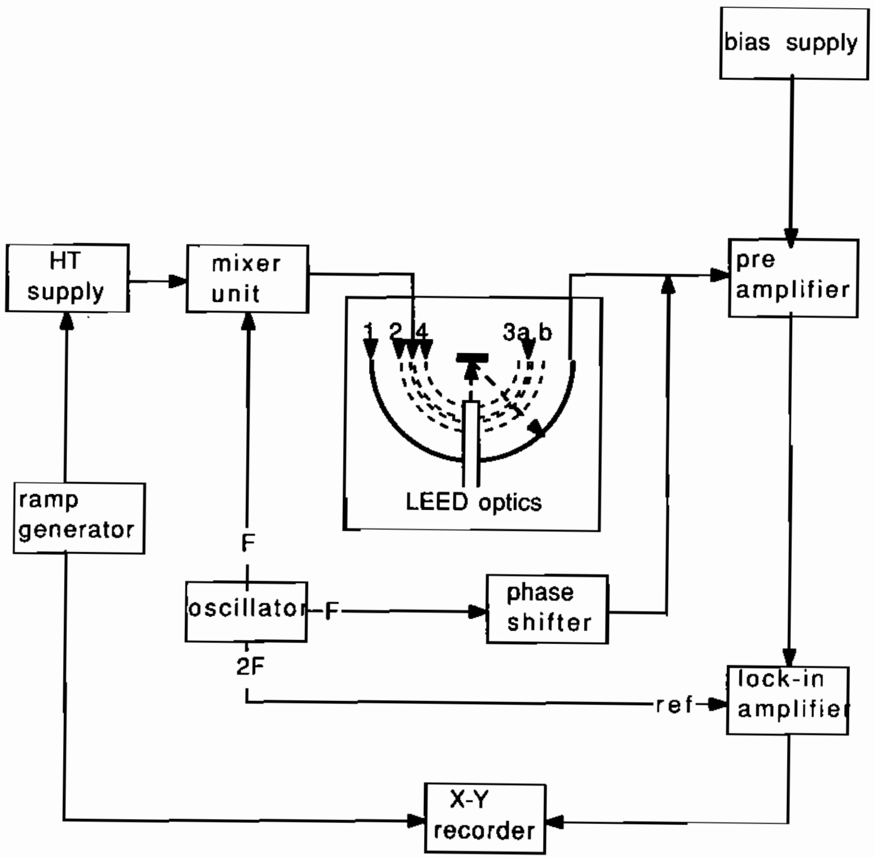

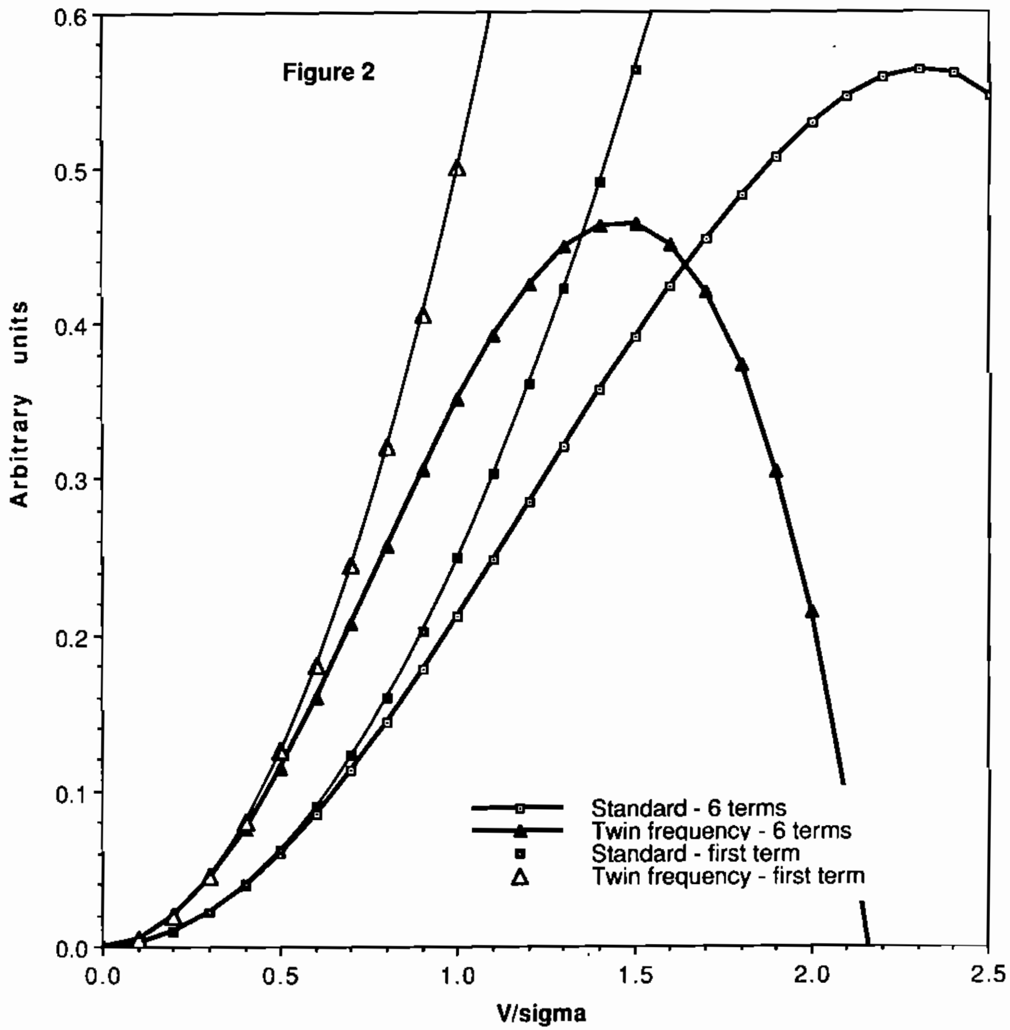

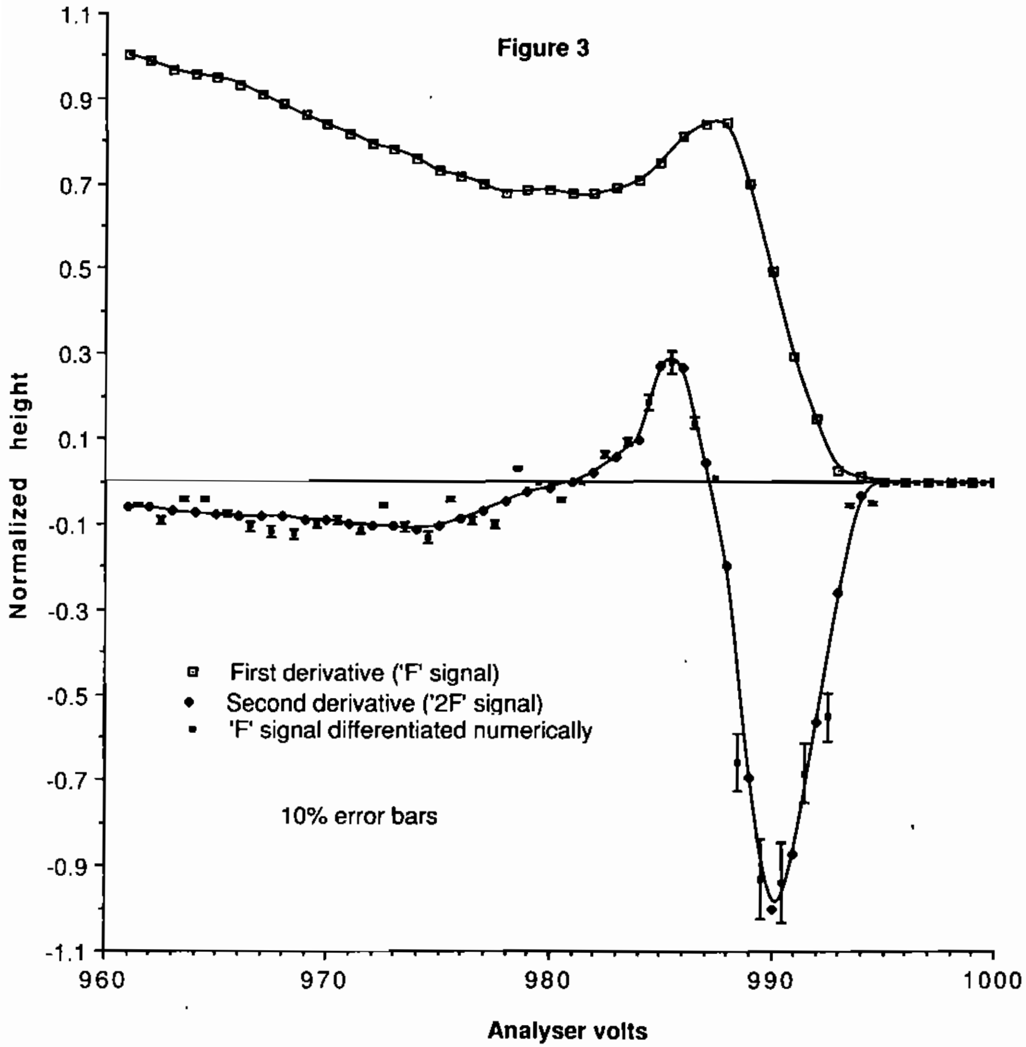

Figure 3
1.1
0.9
0.7
0.5
0.3
0.1
-0.1
-0.3
-0.5
-0.7
-0.9
-1.1
Normalized height
First derivative ('F' signal)
Second derivative ('2F' signal)
'F' signal differentiated numerically
10% error bars
960
970
980
990
1000
Analyser volts

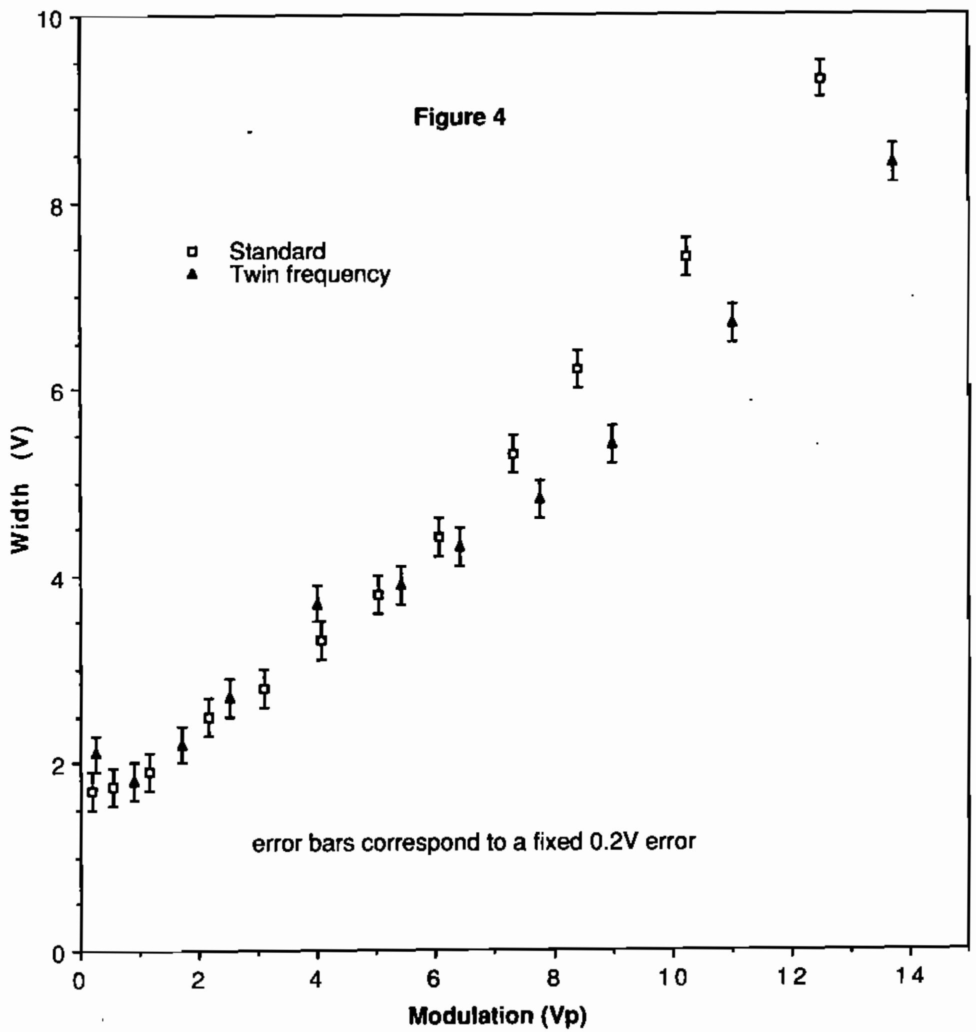

Figure 4
10
8
6
4
2
0
Width (V)
Standard
Twin frequency
error bars correspond to a fixed 0.2V error
0
2
4
6
8
10
12
14
Modulation (Vp)

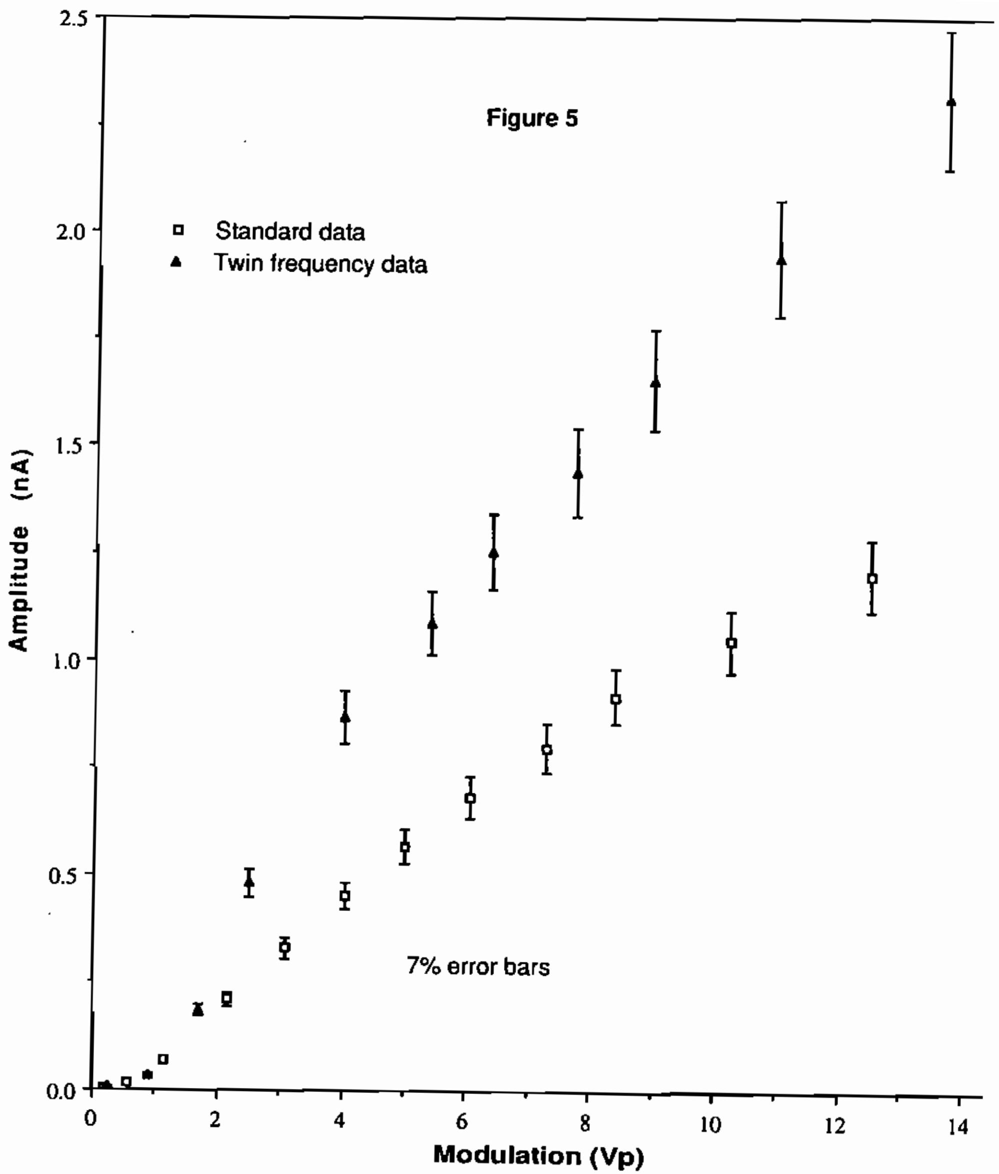

Figure 5
Standard data
Twin frequency data
7% error bars
Amplitude (nA)
Modulation (Vp)
0.0
0.5
1.0
1.5
2.0
2.5
0
2
4
6
8
10
12
14

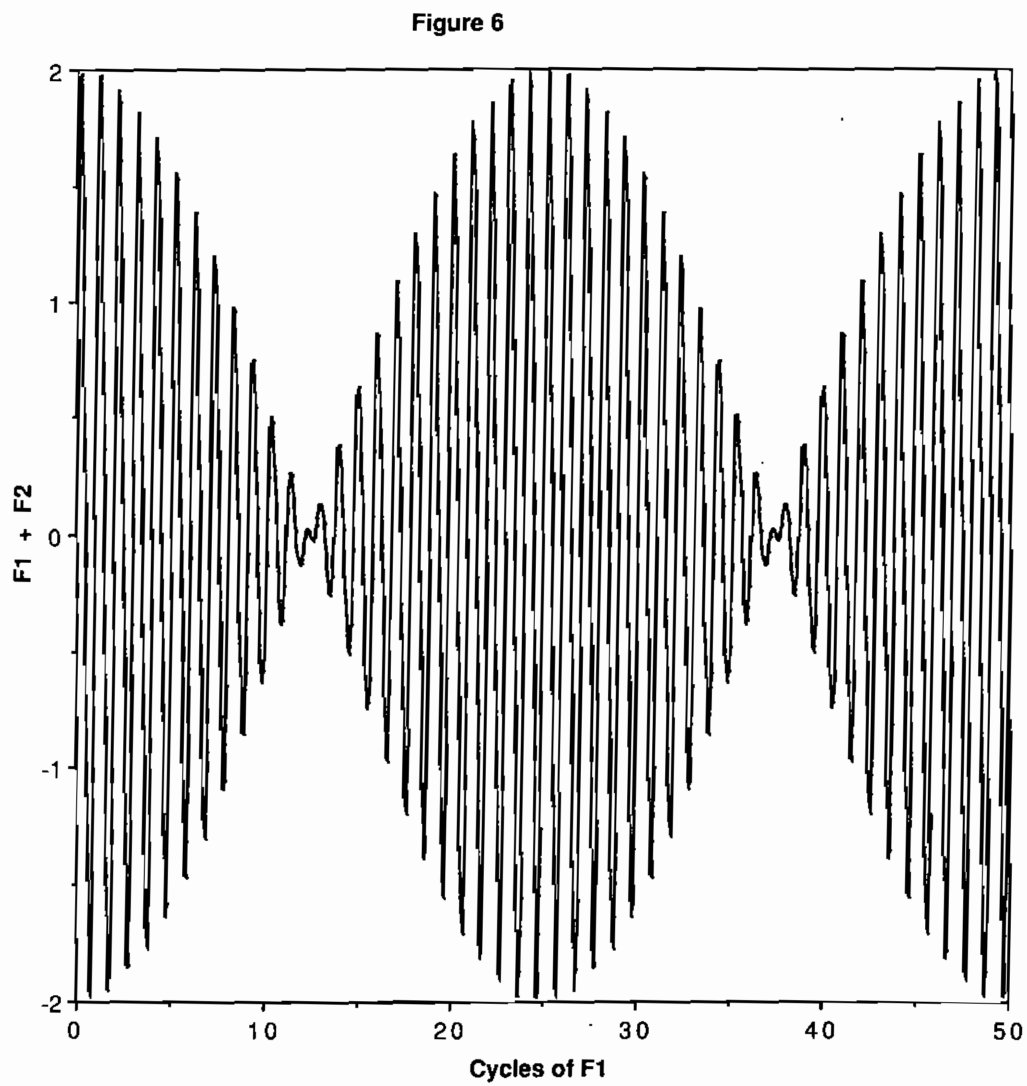

Figure 6
F1 + F2
Cycles of F1
2
1
0
-1
-2
0
10
20
30
40
50

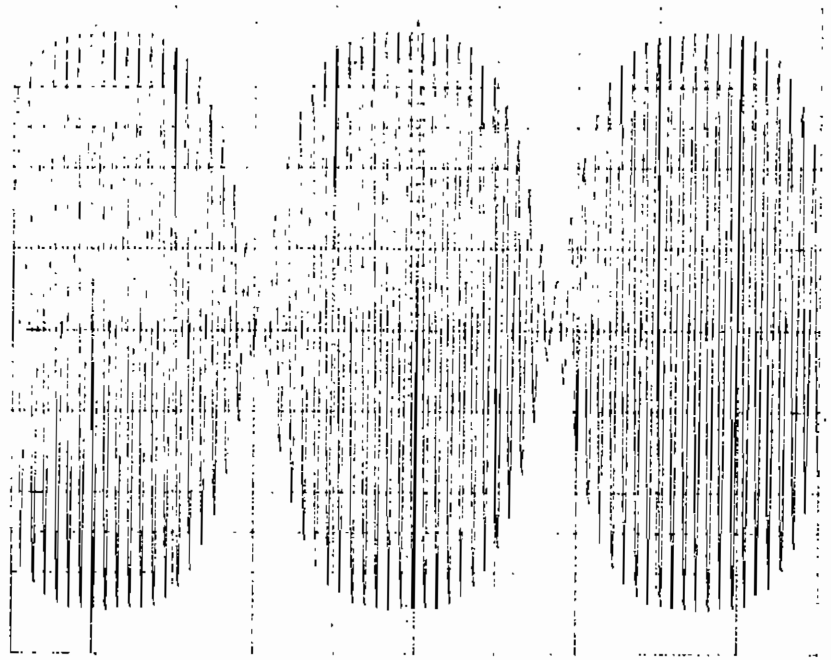

Fig.7

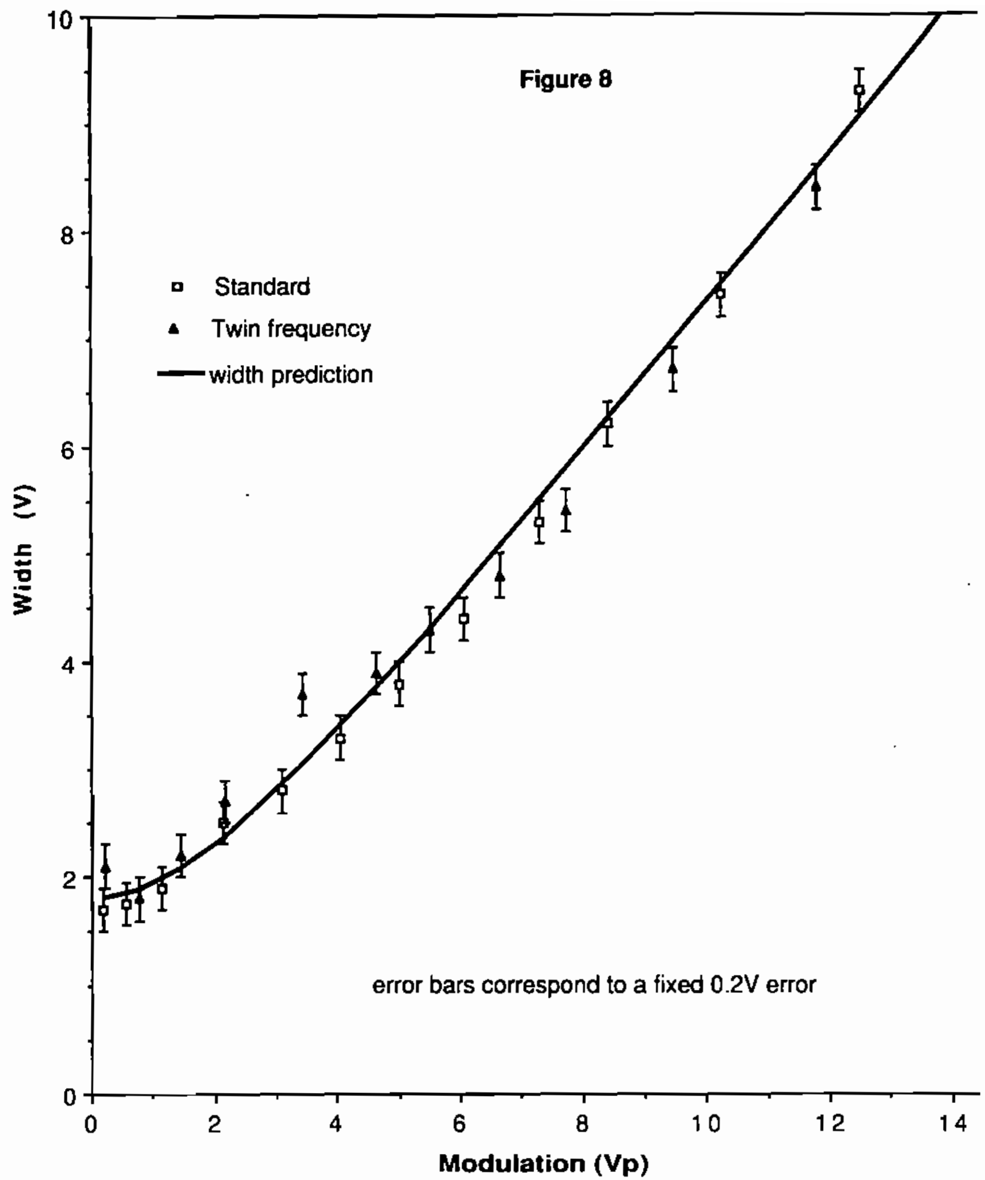
Figure 8
Standard
Twin frequency
width prediction
error bars correspond to a fixed 0.2V error
Width (V)
Modulation (Vp)
0
2
4
6
8
10
0
2
4
6
8
10
12
14

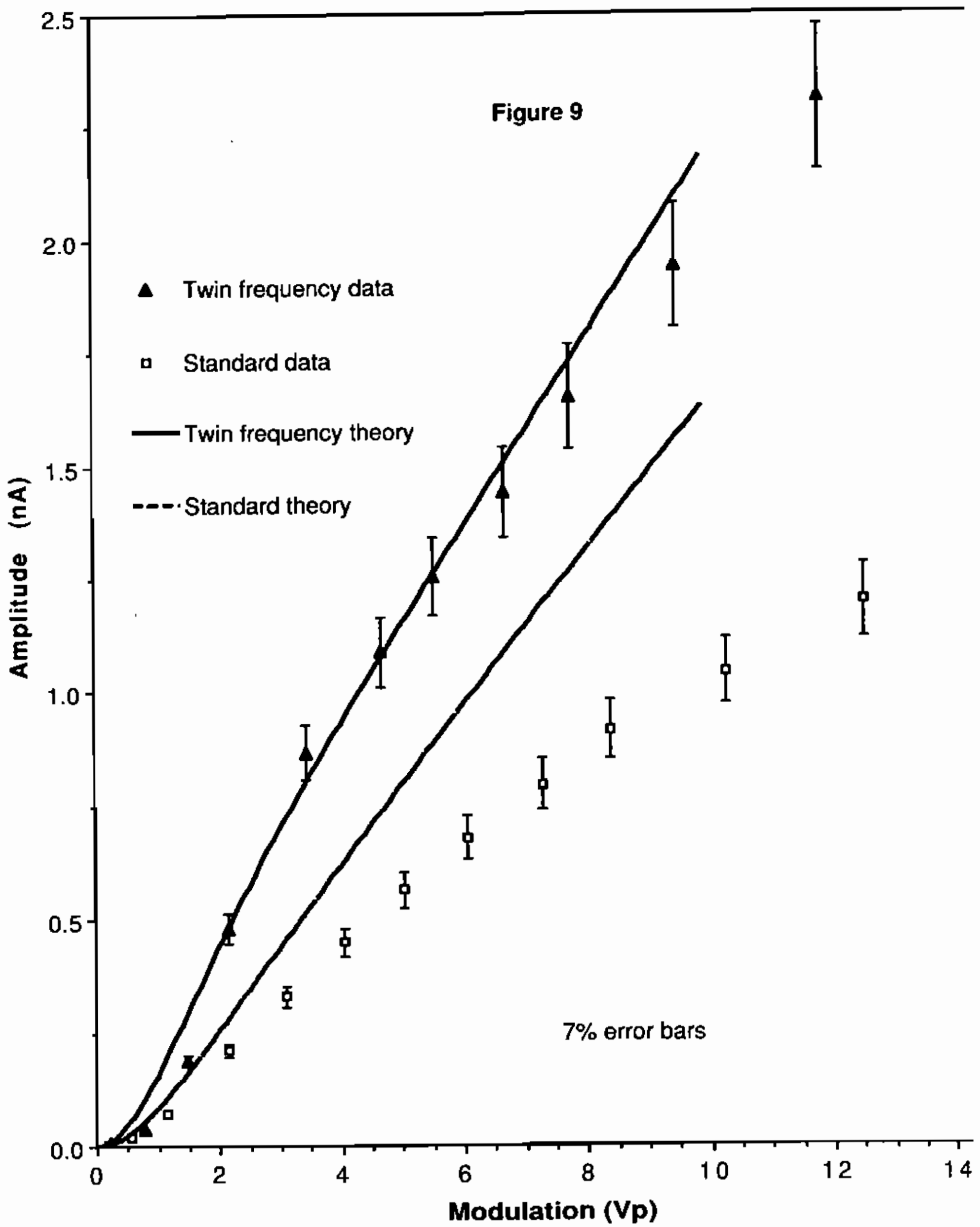

Figure 9
Twin frequency data
Standard data
Twin frequency theory
Standard theory
7% error bars
Amplitude (nA)
Modulation (Vp)
0.0
0.5
1.0
1.5
2.0
2.5
0
2
4
6
8
10
12
14

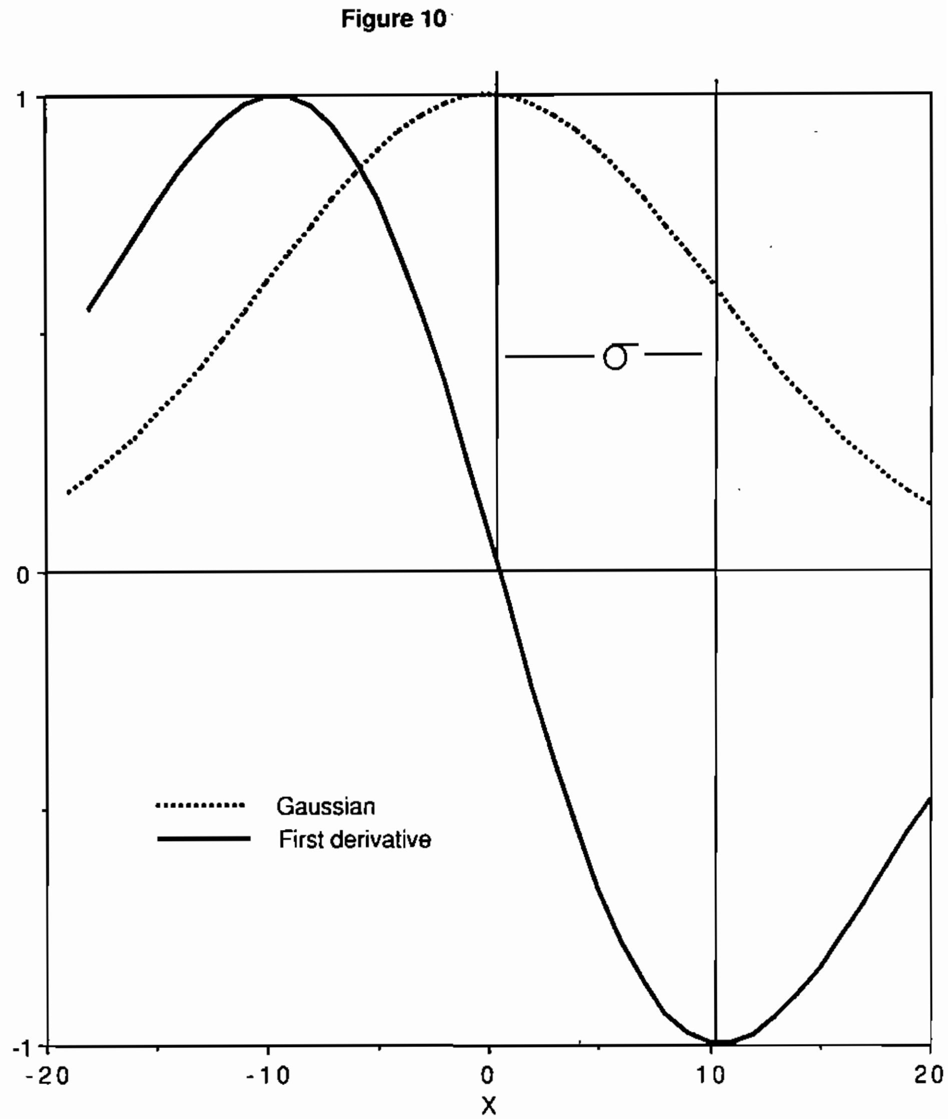

Figure 10
σ
Gaussian
First derivative
X
1
0
-1
-20
-10
0
10
20

Figure 11

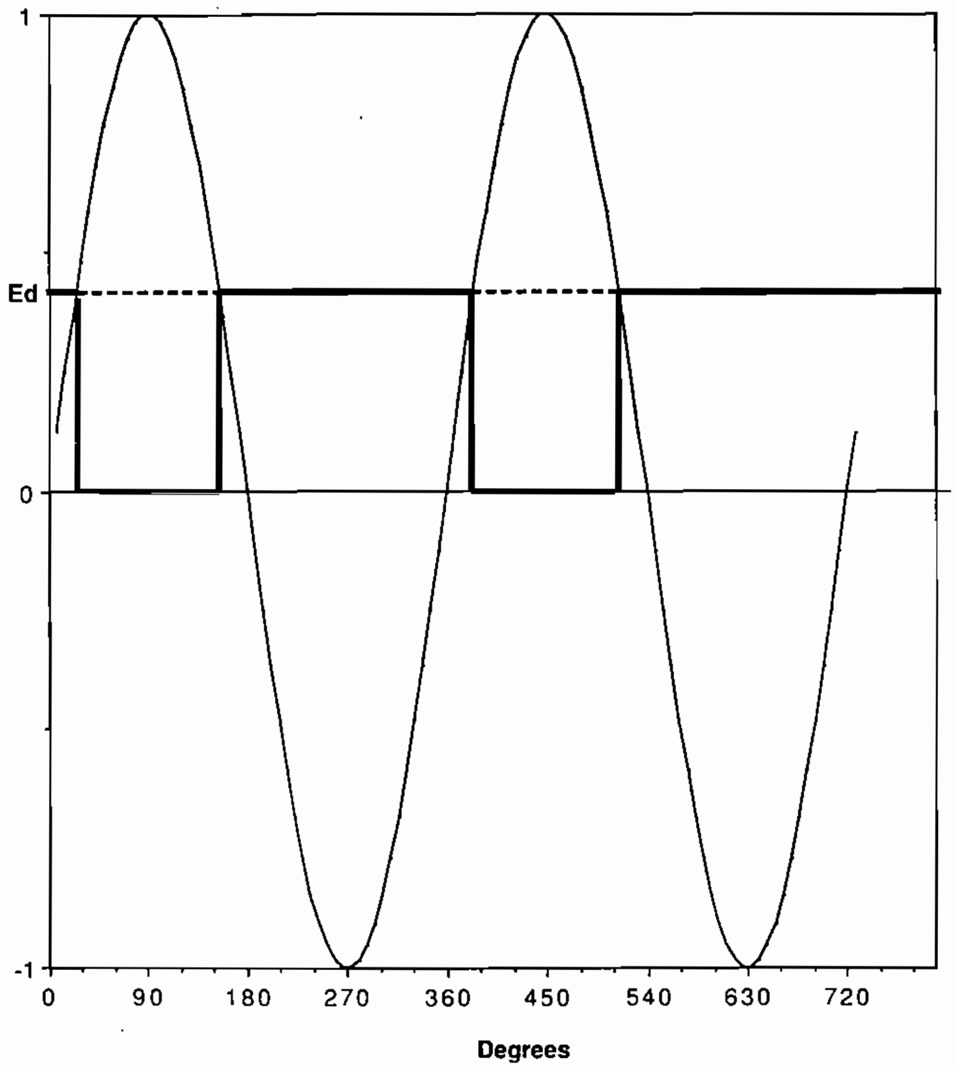

Figure 12

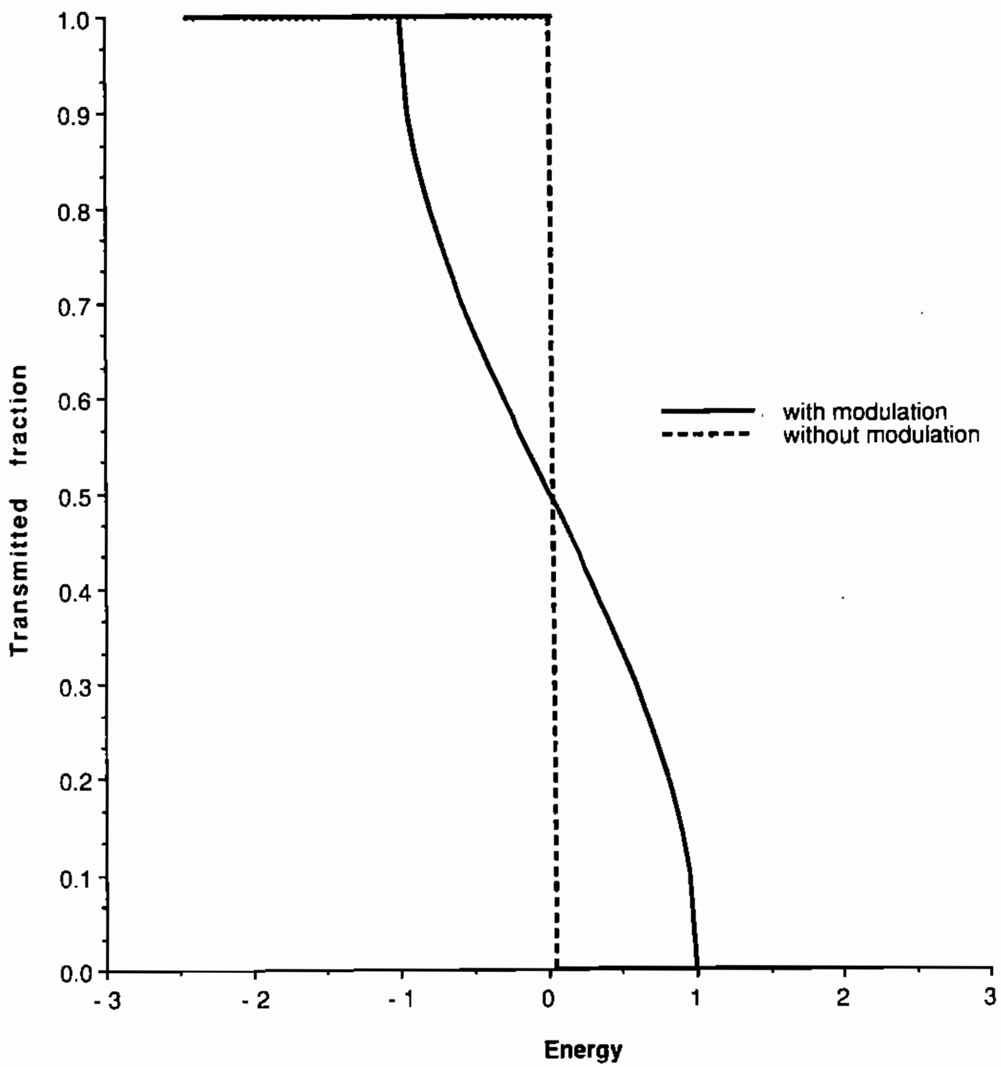

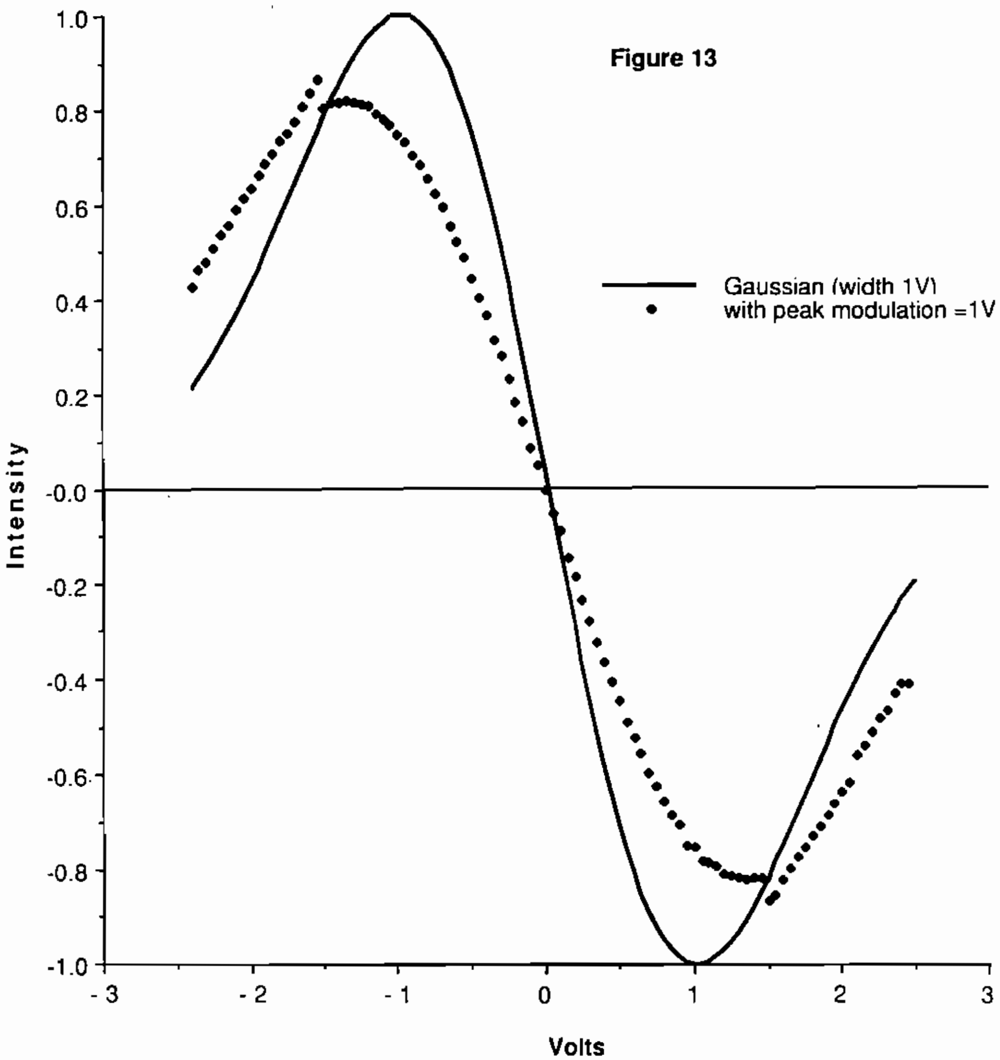
Figure 13
Gaussian (width 1V)
with peak modulation =1V
Intensity
Volts
1.0
0.8
0.6
0.4
0.2
-0.0
-0.2
-0.4
-0.6
-0.8
-1.0
- 3
- 2
- 1
0
1
2
3

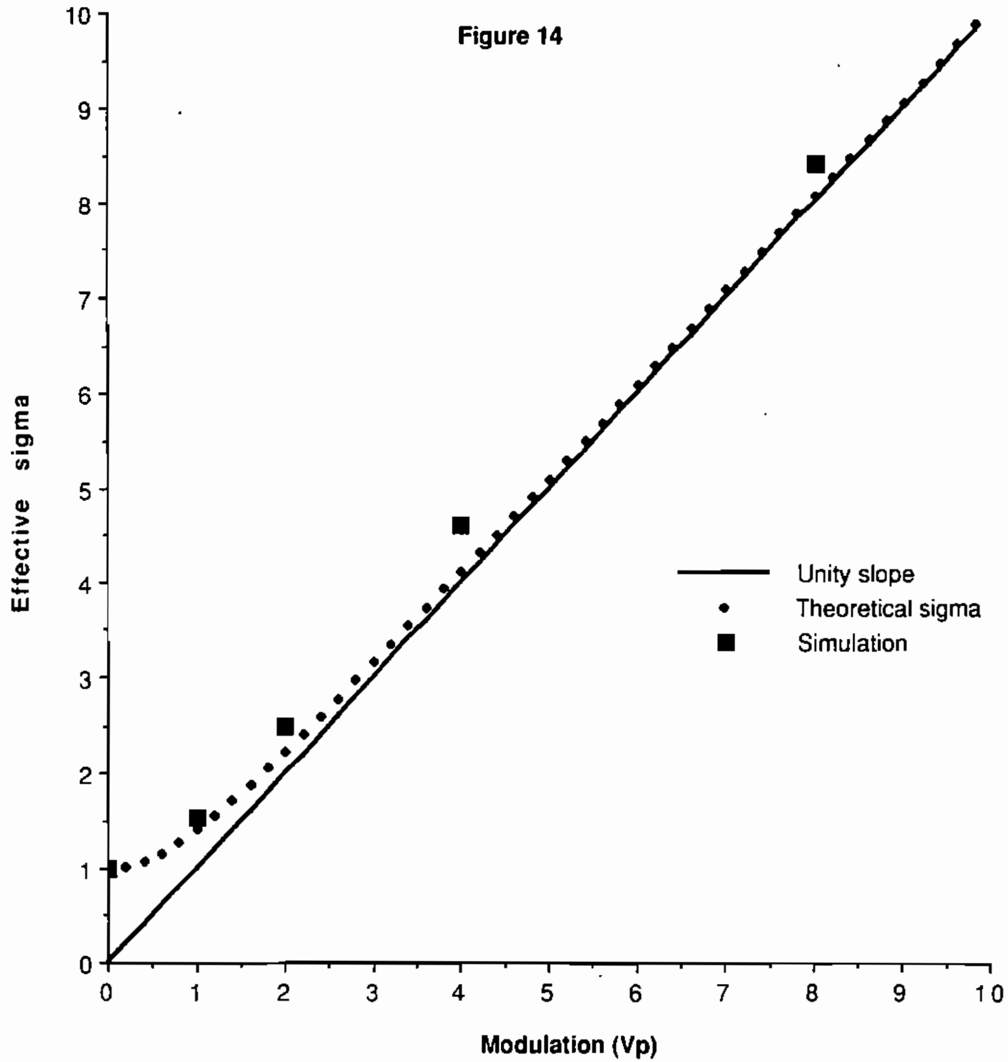
Figure 14
Unity slope
Theoretical sigma
Simulation
Effective sigma
Modulation (Vp)
10
9
8
7
6
5
4
3
2
1
0
0
1
2
3
4
5
6
7
8
9
1 0